

Fast and Accurate Image Registration Using the Multiscale Parametric Space and Grayscale Watershed Transform

Guilherme C.S. Ruppert¹, Fernanda Favretto¹, Alexandre X. Falcão¹, Clarissa Yasuda², Felipe P.G. Bergo^{2*}
 University of Campinas, ¹Institute of Computing and ²Faculty of Medical Sciences
 Campinas, SP, Brazil
 {ruppert, fernandaf, afalcao, clarissa, bergo}@liv.ic.unicamp.br

Abstract— In this work, we propose a new 3D image registration method that uses the grayscale watershed transform to effectively reduce the number of key points needed for registration and a new optimization method that quickly estimates the mapping function using the multiscale parametric space. We validate the method in the context of rigid and intra-subject registration between MR images of the brain, but the method is easily extensible to global deformable registration and other imaging modalities. Extensive experiments have shown that the method is very accurate and provides 3D registration in less than one minute on desktop computers without using any multi-resolution image scheme. We also propose a new color-coding approach for better visualization of the registration differences.

Keywords- *Image Registration, Medical Image Processing, Watershed Lines, Gradient Ascendent Search*

I. INTRODUCTION

Image registration consists of aligning two or more images in a common reference system of spatial coordinates [1]. Medical image registration has been useful to combine data from the same and different imaging modalities, making it possible to visualize changes in anatomy and physiology along time and under different conditions, and to assist image-guided surgery as well as other treatments. This alignment is often done by taking one image domain as reference, transforming corresponding key points from each of the other image domains into the reference system, and then extending this transformation to the remaining pixels. The main problems are the choice of suitable point subsets in each image domain and the determination of their mapping functions onto the reference system. We address both problems in the context of 3D registration between magnetic resonance (MR) images of the human brain. In this application, the methods usually take from a few minutes [2] to several hours [3] to complete registration between two images on a desktop computer. We present an accurate and automatic approach which reduces this time to less than one minute thanks to a grayscale watershed transform [4], used for point subset computation, and a new optimization method used for fast estimation of the mapping function.

We are interested in the problem of intra-subject registration of 3D MR images of the human brain. Our goal is to register pre and post-surgical images from epilepsy patients (mostly children), who had lesioned brain tissues removed to eliminate the foci of the seizures. In the first moment, we want to evaluate the tissue differences between pre- and pos-surgery by using rigid transformation (i.e., without affecting the tissue distribution in the brain) and

understand their relation to cases where the patient continues to suffer seizures after surgery [5].

Therefore, we validate our approach for rigid registration, even though the method is easily extensible to global deformable registration. An additional challenge is that, due to tissue removal, some points do not have correspondents in the reference subset.

II. RELATED WORKS

The literature on the subject is vast. In [6], the authors classify registration methods according to the nature of the registration basis, nature of the transformation, domain of the transformation, user-interaction level, transformation search method, imaging modality, and transformation subject. These seven criteria are further subdivided in some levels as follows. According to the nature of the registration basis, a method can be further classified as object-based or image-based. Object-based methods are those that consider image segmentation (objects, points, lines) to find the transformation [8], while image-based methods avoid segmentation for registration [9, 10]. Methods can also be classified according to the domain of the transformation as global or local. In global approaches, a same transformation is applied to the whole image domain. When different parts of the image have distinct transformations, the method is said local. The transformation search further divides the methods in those based on parameter estimation and parameter search. The former estimates the registration parameters from given point correspondences and the latter determines the parameters by finding an optimum of some criterion function defined in the parameter space [11]. Other well-know terms are also used to classify registration methods: rigid and deformable, interactive and automatic, mono-modal and multi-modal, intra-subject and inter-subject.

The registration method we present here is object-based (we use a grayscale watershed transform to define a reduced subset of registration points), rigid, mono-modal and intra-subject, since we are interested in aligning MR images from a same patient; global, since the transformation for the point subsets is the same for the rest of the image domain; automatic, given that the user only provides the input images; and based on parameter search. Many recent works on registration depend on user interaction [12, 13], are only demonstrated for 2D images [7, 14], provide no quantitative evaluation [13, 7], or are limited to specific applications [2, 3]. The proposed methods often take from a few minutes [2] to several hours [3] to complete the registration of a pair of 3D MR images of the brain on a desktop computer.

* The authors thank to CNPq, CAPES and FAPESP agencies for the financial support provided.

III. METHOD

Let $\hat{I} = (D_I, I)$ and $\hat{J} = (D_J, J)$ be two MR images for registration, where $D_I \subset \mathbb{R}^3$ and $D_J \subset \mathbb{R}^3$ are their image domains and the voxels $p \in D_I$ and $q \in D_J$ have intensities $I(p)$ and $J(q)$, respectively. We aim to find the transformation M , where $D_I = M D_J$, that leads the voxels in D_J to voxels in D_I (reference system) and output the registered image $\hat{R} = (D_I, J)$ with the intensities of \hat{J} in the same domain of \hat{I} .

Let $S_I \subset D_I$ and $S_J \subset D_J$ be subsets of these image domains, such that $S_I = M S_J$. A grayscale watershed transform [4] extracts the subset S_J with voxels that represent relevant borders in the image \hat{J} . These watershed lines are computed from a gradient image $\hat{G}_J = (D_J, G_J)$ of \hat{J} . In the same way, a gradient image $\hat{G}_I = (D_I, G_I)$ of \hat{I} is also computed and we expect that most relevant borders are present in both images. Therefore, we can considerably reduce the problem to find the transformation M that maximizes a criterion function $F(M, S_J, \hat{G}_I)$, where

$$F(M, S_J, \hat{G}_I) = \sum_{\forall q \in S_J, p = Mq \in S_I} G_I(p) \quad (1)$$

The transformation M is then applied to the remaining voxels in D_J to compute \hat{R} .

Despite the reduction from D_J to S_J , we still want to reduce as much as possible the number of candidate transformations M required to maximize $F(M, S_J, \hat{G}_I)$. The next section introduces a new optimization method for this purpose.

A. Search in the Multiscale Parametric Space

In any instance of an image registration problem, the parameters S_J and \hat{G}_I of F are fixed by the instance, and we are searching for an optimal transformation M . We denote by $\hat{\theta} = (\theta_1, \theta_2, \dots, \theta_n)$ the vector of n scalar parameters that compose M . A very often used optimization method is the gradient ascent (or descent, in case of minimization problems) which starts from an initial vector $\hat{\theta}(1)$ and iterates over the equation $\hat{\theta}(t) = \hat{\theta}(t-1) + \eta \nabla F(\hat{\theta})$ with small values of $\eta > 0$ until an iteration no longer increases F .

To reduce the chances of being trapped by local maxima and to speed up the convergence toward the solution, we extend the gradient ascent idea by using a multi-scale scheme, but not in the image space as in typical multi-resolution techniques. Instead we evaluate the gradient in various scales of the parameter space and direct the iteration towards the steepest direction among all scales.

In order to follow the steepest direction, we can substitute $\eta \nabla F(\hat{\theta})$ by a displacement vector.

$$\hat{\theta}(t) = \hat{\theta}(t-1) + (\Delta_1^*, \Delta_2^*, \dots, \Delta_n^*) \quad (2)$$

where $\Delta_i^* \in \{\Delta_i, 0, -\Delta_i\}$, $\Delta_i > 0$, is the displacement that most increases $F(\theta_1, \dots, \theta_i + \Delta_i^*, \dots, \theta_n)$ for

each parameter θ_i , $i = 1, 2, \dots, n$, independently. The method assumes that $F(\theta_1 + \Delta_1^*, \dots, \theta_n + \Delta_n^*)$ increases too. For each scale $j = 1, 2, \dots, m$, we must iterate over all parameters choosing the displacement $\Delta_i^* \in \{\Delta_i(j), 0, -\Delta_i(j)\}$ that most increases $F(\theta_1, \dots, \theta_i + \Delta_i^*, \dots, \theta_n)$. The displacements $\Delta_i(j) > 0$ increase as we reduce the scale of the parameter space and must be specified for each application of the method. These displacements are actually specified by two arrays $W = (W_1, W_2, \dots, W_n)$ and $\Delta = (\Delta_1, \Delta_2, \dots, \Delta_n)$, where W_i specifies the maximum value for each parameter i and Δ_j specifies a scale j in terms of a percentage of the values in the array W . Algorithm 1 shows a pseudo-code of this procedure.

Algorithm 1 OPTIMIZATION ALGORITHM

INPUT: Array θ of starting parameters, Array Δ with the scales and Array W with the parameters maximum values.
 OUTPUT: Array θ^* with the best parameters.
 AUXILIARY: Array Δ^* ; scalars $V_F^*, V_F, V_{F0}, V_{F1}$ and V_{F2}

```

1.  $V_F^* \leftarrow F(\theta[1], \dots, \theta[n])$ 
2. For  $i \leftarrow 1$  to  $n$  do  $\theta^*[i] \leftarrow \theta[i]$ 
3. do
4.    $V_{F0} \leftarrow V_F^*$ 
5.   For  $i \leftarrow 1$  to  $n$  do  $\theta[i] \leftarrow \theta^*[i]$ 
6.   For  $j \leftarrow 1$  to  $m$  do
7.     For  $i \leftarrow 1$  to  $n$  do
8.        $V_F \leftarrow V_{F0}$  e  $\Delta^*[i] \leftarrow 0$ 
9.        $V_{F1} \leftarrow F(\theta[1], \dots, \theta[i] + \Delta[j] * W[i], \dots, \theta[n])$ 
10.       $V_{F2} \leftarrow F(\theta[1], \dots, \theta[i] - \Delta[j] * W[i], \dots, \theta[n])$ 
11.      if  $V_{F1} > V_F$  then  $V_F \leftarrow V_{F1}$  e  $\Delta^*[i] \leftarrow \Delta[j] * W[i]$ 
12.      if  $V_{F2} > V_F$  then  $\Delta^*[i] \leftarrow -\Delta[j] * W[i]$ 
13.       $V_F \leftarrow F(\theta[1] + \Delta^*[1], \dots, \theta[n] + \Delta^*[n])$ 
14.      if  $V_F > V_F^*$  then
15.         $V_F^* \leftarrow V_F$ 
16.        For  $i \leftarrow 1..n$  do  $\theta^*[i] \leftarrow \theta[i] + \Delta^*[i]$ 
17.    While  $V_F^* > V_{F0}$ 
    
```

B. Registration Procedure

The images used in this work are volumetric T1-weighted MR images. Image resolutions are either 0.98 x 0.98 x 1.0 mm or 0.98 x 0.98 x 1.5 mm. MR intensities range from 0 to 4095 and image sizes range from 256x256x100 to 256x256x160. The first step performed before registration is the interpolation of both images to an isotropic voxel size with the minimum value among all voxel dimensions.

Next we normalize intensities of both images by linearly mapping the intensities between the 1% and 99% marks of the accumulated histogram to the [0, 4095] interval. This prevents high intensity MR artifacts, notably those from blood vessels, from forming strong borders. The watershed lines [4] in $\hat{G}_J = (D_J, G_J)$ are computed with an Image Foresting Transform (IFT) [15], which requires the specification of two parameters: a non-reflexive adjacency relation A between nearby voxels in D_J and a path-cost function that assigns a value to any sequence of adjacent voxels. We use 26-neighborhood as adjacency relation and path-cost function $f(\pi_p)$ for a sequence of voxels $\pi_p = \langle p_1, p_2, \dots, p \rangle$ with terminus p .

$$f(\pi_p) = \max\{G_J(p_1) + K, G_J(p_2), \dots, G_J(p)\} \quad (3)$$

where $G_j(p)$ is the gradient computed for a voxel p as proposed in [16], $K = 0.07G_{\max}$ for a maximum gradient value G_{\max} in the image, and the factor 0.07 was determined empirically. The IFT segments the image into homogeneous regions and the watershed lines are the borders between these regions. These images are shown in Figure 1.

For registration, we want to find a transformation M that optimizes the matching of the watershed lines S_j to their counterparts in \hat{G}_i , using (1), where \hat{G}_i is the gradient proposed in [16]. For M to be a rigid transformation, we state it as a composition of one translation and three rotations. The transformation M can then be defined by 6 scalar parameters: $\hat{\theta} = (R_x, R_y, R_z, T_x, T_y, T_z)$, where R_x, R_y, R_z define the rotations (angles, in degrees) and T_x, T_y, T_z define the translations (displacements, in mm). MR images provide information about the orientation of the patient. Thus, images \hat{I} and \hat{J} are provided in the same orientation, so we can safely start the search from $\hat{\theta} = \{0, 0, 0, 0, 0, 0\}$ as initial parameters and registration is performed by using Algorithm 1 to maximize F with M being the identity matrix as starting point. The arrays used to specify the displacements were $\Delta = (10\%, 6\%, 3\%, 0.5\%, 0.05\%)$ and $W = (180, 180, 180, D_x/2, D_y/2, D_z/2)$, where D_x, D_y and D_z are the dimensions of the image in mm along the corresponding axes. At each iteration, the method evaluates positive and negative variations of $\Delta[j]*W[i]$ for each parameter i and scale j . This represents variations in rotation from $\pm 0.09^\circ$ to $\pm 18^\circ$ and variations in translation from $\pm 0.13\text{mm}$ to $\pm 25.6\text{mm}$, when $D_{x,y,z} = 256\text{mm}$.

IV. EXPERIMENTS AND RESULTS

We evaluated the registration accuracy of the proposed method in four sets of experiments. In the first set we used MR-T1 images from control subjects transformed by known rigid transforms. In the second set, we used the same control images, but added synthetic (phantom) lesions to the image being registered. In the third set, we added noise to the control images to measure robustness to noise. In the fourth set we used pairs of clinical MR-T1 images from patients who underwent brain surgery, acquired before and after surgery.

In the first set of experiments we used 20 images from healthy control subjects. For each reference image we created 10 new images by applying random rigid transformations with rotation varying from -20° to 20° around all axes and translations varying from -20mm to 20mm along all axes. We then applied the proposed registration method between each of the 20 images and its 10 counterparts, performing a total of 200 registration tasks. Registration succeeded on all cases with negligible errors. Table 1 shows the mean, standard deviation and maximum values of the rotation and translation errors.

Table 1. Error measurements on the first three sets of experiments (200 image pairs each).

	Rotation Error (Deg.)			Translation Error (mm)		
	Mean	σ	Max	Mean	σ	Max
Set 1	0.04	0.02	0.09	0.51	0.05	0.62
Set 2	0.05	0.03	0.16	0.51	0.06	0.67
Set 3	0.05	0.04	0.19	0.54	0.09	0.74

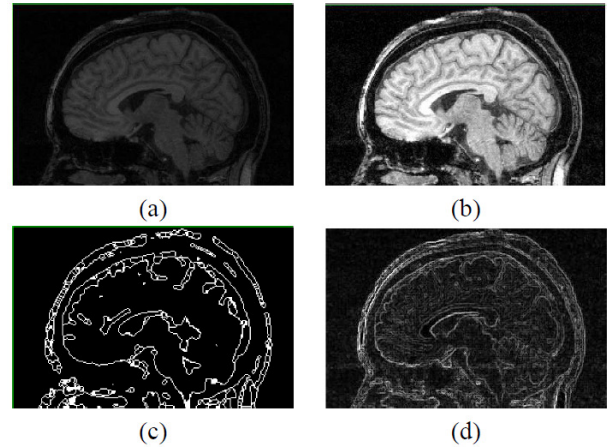


Fig. 1. Sample MR-T1 slice and the preprocessing steps: (a) Original slice. (b) After intensity Normalization. (c) Watershed lines from (b). (d) Gradient of (b). The accumulation of gradient intensities along the watershed lines is the criteria for registration optimality.

In the second set of experiments we used the same 20 images from the previous experiment set, but a synthetic artifact mimicking a large surgical cavity was added to the images being registered. Then we applied 10 random rigid transformations to each of the 20 images with synthetic lesions and registered them to their respective original control image without lesion, performing a total of 200 registration tasks. Registration succeeded with negligible errors in all cases. The results are shown on Table 1.

To evaluate the robustness of the method with respect to noise, we used 20 control images and added zero-mean Gaussian noise with $\text{SNR}=5\text{dB}$, which represents a high level of degradation to the image. The previous experiment was repeated with noise added and, even subject to such a high level of noise, the method performed with no noticeable impact to the accuracy, as shown on Table 1 for set 3.

To evaluate our method on real clinical images, we used a dataset of 45 pairs (pre and post surgery) of MR-T1 images from epilepsy patients where part of the brain tissue was removed. In this fourth set of experiments, it was not possible to perform a quantitative evaluation, since no ground-truths were available. However, it is possible to evaluate the quality of the registration result through visual inspection by an expert using special visualization techniques. The most used technique is the mosaic scheme, where the fixed image and the registered image are displayed at the same time in a checkerboard mosaic. The problem is that this scheme doesn't reveal small differences clearly.

In this work, we introduce a new technique using color coding. Both images are normalized and then combined by assigning the red channel to one image and the green channel to the other. The blue channel is filled with the average of both images. In this scheme, the regions with accurate registration appear in unsaturated gray, while red- or green-hued regions reveal intensity mismatches. When the registration is accurate, few saturated voxels are seen outside the surgery area. Naturally, clinical aspects have to be taken into account, such as the swelling of regions around the removed tissue. Figure 2 illustrates this technique of visualization for two cases.

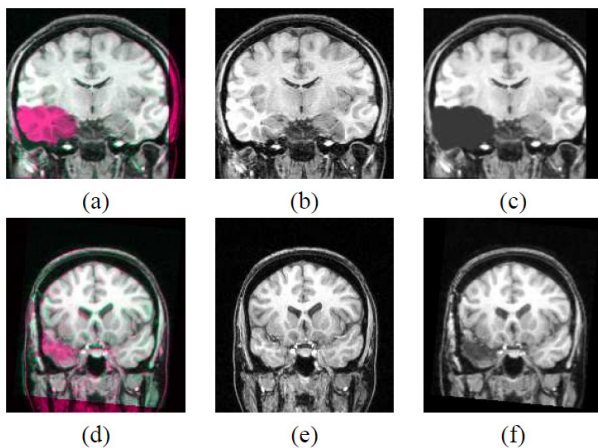


Fig. 2. Visualization of registration using color coding. The first column shows the combination between the fixed image (second column) and the registered moving image (third column). The first row shows an example of a synthetic lesion case. The second row is an example of clinical image (pre and post-surgery).

Visual inspection of all 45 cases by a neurosurgeon expert showed that the registration method was successful on all cases. The greenish and reddish parts indicate gain and loss of signal intensity, respectively.

The method was implemented in C language and takes less than 40 seconds for a typical MR image (256x256x160) on a Intel Core-Duo2 E6750 2.66GHz 4GB RAM machine. Most of this time is spent on the computation of gradient and watershed lines (around 32 seconds) and the registration itself takes less than 8 seconds.

To have a comparative idea, we have implemented a typical rigid registration method using gradient descent optimizer and mean squared pixel-wise difference metric using the ITK library. We repeated experiments 1 and 2. The method took 23 minutes on average to register each image, which is 35 times slower than the proposed method, and the descent gradient took 26% more iteration than our method to find the solution, which evidences that our multi-scale approach converges in less steps. The visual inspection using the color coding showed that both methods achieved good registration with practically no visible saturated voxels. We haven't performed a deep quantitative analysis but this will be done in the future.

V. CONCLUSION AND FUTURE WORKS

We proposed and validated a new approach for 3D rigid registration between MR images of the human brain obtained from a same subject. The method can be extended to other imaging modalities and global deformable registration, by finding a suitable gradient image to obtain watershed lines and adding scaling factors to the transformation M . The grayscale watershed transform was used to effectively reduce the subset of key points for registration while a new optimization method was proposed to quickly estimate M . This method can also be applied to other optimization problems by specifying which parameters θ_i affect the criterion function F . The experiments involved 645 registration tasks with images of control subjects and patients, before and after surgery, and images with synthetic lesions and noise. The results show that the method is fast and as accurate as the image resolutions allow. Also the proposed color-coding

visualization approach showed to be a very good tool for registration evaluation.

Future works include a deep evaluation and comparison of the proposed method against other methods in the literature, evaluation of the method for global deformable registration, image registration between distinct modalities, and the extension of the optimization method to other image analysis problems.

REFERENCES

- [1] J.V. Hajnal, D. L. G. Hill, and D. J. Hawkes, *Medical Image Registration*, CRC Press, London, 2001.
- [2] Z. Lu, Q. Feng, P. Shi, and W. Chen, "A fast 3-D medical image registration algorithm based on equivalent meridian plane," *Image Processing*, vol. 5, pp. 357–360, 2007.
- [3] J. Han, M. Qiao, J. Hornegger, T. Kuwert, W. Bantz, and W. Romer, "Automatic sub-volume registration by probabilistic random search," *Medical Imaging - Image Processing - Proceedings of SPIE*, vol. 6144, pp. 799–807, 2006.
- [4] R.A. Lotufo, A.X. Falcão, and F. Zampiroli, "IFT-Watershed from gray-scale marker," in *Proc. of XV Brazilian Symp. on Computer Graphics and Image Processing*, Oct 2002, pp. 146–152, IEEE.
- [5] C. L. Yasuda, C. C. Valise, A. V. Saude, A. L. F. Costa, F. R. Pereira, M. Morita, L. E. Betting, H. Tedeschi, E. Oliveira, G. Castellano, and F. Cendes, "Recovery of white matter atrophy (WMA) after successful surgery in mesial TLE," in *Proc. 60th Annual Meeting of the American Academy of Neurology*, Chicago, IL, 2008, p. A4.
- [6] J. B. A. Maintz and M. A. Viergever, "A survey of medical image registration," *Medical Image Analysis*, vol. 2, no. 1, pp. 1–36, 1998.
- [7] X. Zou, X. Zhao, and Y. Feng, "An efficient medical image registration algorithm based on gradient descent," *Complex Medical Engineering*, pp. 636 – 639, May 2007.
- [8] J. Feldmar, G. Malandain, J. Declerck, and N. Ayache, "Extension of the icp algorithm to non-rigid intensity-based registration of 3d volumes," in *Mathematical methods in biomedical image analysis*, pp. 84–93. IEEE computer society press, Los Alamitos, CA, 1996.
- [9] P. Viola and W. M. Wells, "Alignment by maximization of mutual information," *International Journal of Computer Vision*, vol. 24, no. 2, pp. 137–154, Sep 1995.
- [10] F. Maes, A. Collignon, D. Dandekermeulen, G. Marchal, and P. Suetens, "Multimodality image registration by maximization of mutual information," *IEEE Transactions in Medical Imaging*, vol. 16, pp. 187–198, 1997.
- [11] D. Vandermeulen, F. Maes, and P. Suetens, "Comparative evaluation of multiresolution optimization strategies for multimodality image registration by maximization of mutual information," *Medical Image Analysis*, vol. 3, no. 4, pp. 373–386, 1999.
- [12] U. Pietrzyk, K. Herholz, G. Fink, A. Jacobs, R. Mielke, I. Slansky, M. Wurker, and W-D. Heiss, "An interactive technique for three-dimensional image registration: validation for PET, SPECT, MRI and CT brain studies," *Journal of Nuclear Medicine*, vol. 35, no. 12, pp. 2011–2018, 1994.
- [13] C. Huang, C. Jiang, and W. Sung, "Medical image registration and fusion with 3d ct and mr data of head," *Computer-Based Medical Systems*, pp. 401 – 404, 2006.
- [14] H. H. Wen, W. C. Lin, and C. T. Chen, "Knowledge-based medical image registration," *Engineering in Medicine and Biology Society*, vol. 3, pp. 1200 – 1201, Nov 1996.
- [15] A. X. Falco, J. Stolfi, and R. A. Lotufo, "The image foresting transform: Theory, algorithms and applications," *IEEE Trans. on Pattern Analysis and Machine Intelligence*, vol. 26, no. 1, pp. 19–29, Jan 2004.
- [16] F. P. G. Bergo, A. X. Falcão, P. A. V. Miranda, and L. M. Rocha, "Automatic image segmentation by tree pruning," *J Math Imaging and Vision*, vol. 29, no. 2–3, pp. 141–162, Nov 2007.